Journal of Physics: Conference Series **527** (2014) 012018 doi:10.1088/1742-6596/527/1/012018

Elliptic flow and shear viscosity of the shattered color glass condensate

Marco Ruggieri

Department of Physics and Astronomy, University of Catania, Via S. Sofia 64, I-95125 Catania

E-mail: marco.ruggieri@lns.infn.it

Francesco Scardina, Salvatore Plumari, Vincenzo Greco

Department of Physics and Astronomy, University of Catania, Via S. Sofia 64, I-95125 Catania
INFN-Laboratori Nazionali del Sud, Via S. Sofia 62, I-95123 Catania, Italy

Abstract. In this contribution, we report on our results about the computation of the elliptic flow of the quark-gluon-plasma produced in relativistic heavy ion collisions, simulating the expansion of the fireball by solving the relativistic Boltzmann equation for the parton distribution function tuned at a fixed shear viscosity to entropy density ratio η/s. We emphasize the role of saturation in the initial gluon spectrum modelling the shattering of the color glass condensate, causing the initial distribution to be out of equilibrium. We find that the saturation reduces the efficiency in building-up the elliptic flow, even if the thermalization process is quite fast $\tau_{therm} \approx 0.8\,\mathrm{fm/c}$. and the pressure isotropization even faster $\tau_{isotr} \approx 0.3\,\mathrm{fm/c}$. The impact of the initial non-equilibrium manifests for non-central collisions and can modify the estimate of the viscosity respect to the assumption of full thermalization in p_T-space.

1. Introduction

In the last decade it has been reached a general consensus that ultra-relativistic heavy-ion collisions (uRHICs) at the Relativistic Heavy-Ion Collider (RHIC) and the Large Hadron Collider (LHC) create a hot and dense strongly interacting quark and gluon plasma (QGP) [1, 2, 3, 4]. A main discovery has been that the QGP has a very small shear viscosity to entropy density ratio, η/s, which is more than one order of magnitude smaller than the one of water [5, 6], and close to the lower bound of $1/4\pi$ conjectured for systems at infinite strong coupling [7]. A key observable to reach such a conclusion is the elliptic flow [8], $v_2 = \left\langle (p_x^2 - p_y^2)/(p_x^2 + p_y^2) \right\rangle$. In fact, the expansion of the created matter generates a large anisotropy of the emitted particles that can be primarily measured by v_2. The origin of v_2 is the initial spatial eccentricity, $\epsilon_x = \langle y^2 - x^2 \rangle / \langle x^2 + y^2 \rangle$ of the overlap region in non-central collisions, which is responsible for different pressure gradients in the transverse plane thus favoring flow preferably along the x direction rather than y direction. The observed large v_2 is considered a signal of a very small η/s because if η/s was large then viscosity would damp the flow, hence reducing anisotropy in momentum space. Calculations agree in indicating an average η/s of the QGP lying in the range $4\pi\eta/s \approx 1 - 3$ [9, 10, 11, 12, 13, 14, 15, 16, 17, 18, 19, 20].

Along with the existence of a deconfined QGP matter and the understanding of its properties, the uRHIC program offers the opportunity to verify the picture in which the two colliding

nuclei are described as two sheets of Color Glass Condensate (CGC) [21]. The CGC would be generated by the very high density of the gluon distribution function at low x (parton longitudinal momentum fraction), which triggers a saturation of the distribution for p_T below a saturation scale, Q_s. The determination of the shear viscosity η/s of the QGP and the search for the CGC are related: in fact the uncertainty on the initial condition translates into an uncertainty on the theoretical estimate of η/s [11, 22, 23, 24].

In this contribution we report our results [19, 25] about the computation of the elliptic flow of the quark-gluon-plasma produced in relativistic heavy ion collisions, simulating the expansion of the fireball by solving the relativistic Boltzmann equation for the parton distribution function tuned at a fixed shear viscosity to entropy density ratio η/s [17, 18, 25, 26, 27]. The advantage of using kinetic theory is that starting from a one-body phase space distribution function $f(x,p)$, and not from the energy-momentum tensor $T^{\mu\nu}$, it is straightforward to initialize simulations from a non-equilibrium distribution function, while hydrodynamics relies on the gradient expansion of the stress tensor and therefore is applicable only if initial deviations from local equilibrium are small.

In this study we will consider several kinds of initial conditions, two of them related to the shattering of the CGC which takes place after the collision. For describing the latter we make use of the KLN model [28, 29, 30, 31, 32], which has been largely employed to study the dynamics of HIC and the viscosity of the QGP within hydrodynamical simulations [11, 24, 22, 31, 33, 34, 35]. The uncertainty in the initial condition translates into an uncertainty on η/s of at a least a factor of two as estimated by mean of several viscous hydrodynamical approaches [24, 22, 11, 23]. We point out that the implementation of the shattered CGC initialization in hydrodynamics takes into account only the different space distribution respect to a geometric Glauber model, discarding the key and more peculiar feature of the damping of the distribution for p_T below the Q_s saturation scale. We have found by mean of kinetic theory that this has a significant impact on the build-up of v_2, hence on the determination of η/s.

In our study we neglect the initial time evolution of the chromo-electric and chromo-magnetic fields (the glasma) produced immediately after the collision. According to the commonly accepted picture of heavy ion collisions, our approach should be justified as soon as the initial strong fields decay into particle quanta. Characteristic time for the glasma decay is of the order of $\tau_0 \approx 1/Q_s$, which turns out to be of the order of a fraction of fm/c [36, 37, 38]. From this time on the field contribution to the pressure is less important, and the dynamics is dominated by the scatterings among partons, which justifies the use of kinetic theory to describe the sequent evolution of the system. The advantage to use kinetic theory from τ_0 rather than hydro is that the nonequilibrium initial distribution is not problematic as kinetic theory is built to study the evolution of a generic $f(x,p)$ distribution function.

2. Initial conditions for the simulations

In this section we specify the initial conditions we implement in our simulations. The first one is based on the Glauber model, see [39] for a review, with an $\boldsymbol{x}$-space distribution given by the a standard mixture $0.85N_{part} + 0.15N_{coll}$ and a $\boldsymbol{p}$-space thermalized spectrum in the transverse plane at a time $\tau_0 = 0.6\,\mathrm{fm/c}$ for the RHIC runs and $\tau_0 = 0.3$ fm/c for the LHC runs. Maximum temperature is assumed $T_0 = 0.34$ GeV for the Au-Au collisions at RHIC energy and $T_0 = 0.51$ GeV for the Pb-Pb collisions at LHC energy. We also assume $y = \eta$ at $\tau = \tau_0$, where η corresponds to space-time rapidity; we also assume boost invariance in the longitudinal direction at $\tau = \tau_0$ which implies independence of the initial distribution on y. Following the nomenclature introduced in [19, 25] we will refer to this case as Th-Glauber.

The other two kinds of initial conditions we use in our simulations [19, 25] are based on a model of gluon production for the shattered CGC named factorized-KLN (fKLN in the

following) [28, 30, 31], in which the initial spectrum is assumed to be

$$\frac{dN}{dyd^2\boldsymbol{x}_\perp d^2\boldsymbol{p}_T} = \kappa \frac{p_A p_B}{p_T^2} \int^{p_T} d^2\boldsymbol{k}_T \alpha_S(Q^2) \phi_A(x_1, k_T^2; \boldsymbol{x}_\perp) \phi_B(x_2, (\boldsymbol{p}_T - \boldsymbol{k}_T)^2; \boldsymbol{x}_\perp) \; ; \qquad (1)$$

the coordinate space distribution is obtained by integration of the above equation over $\boldsymbol{p}_T$. Here $(\boldsymbol{p}_T, y)$ correspond to transverse momentum and momentum rapidity of the produced gluons respectively, and $x_{1,2} = p_T \exp(\pm y)/\sqrt{s}$. In equation (1) $p_{A,B}$ denote the probability to find one nucleon at a given transverse coordinate, $p_A(\boldsymbol{x}_\perp) = 1 - [1 - \sigma_{in} T_A(\boldsymbol{x}_\perp)/A]^A$ where σ_{in} is the inelastic cross section and T_A corresponds to the usual thickness function of the Glauber model. The overall constant κ in equation (1) is fixed in order to reproduce the experimental multiplicity in the most central collisions.

The specific form of the unintegrated gluon distribution function for gluons $\phi_{A,B}$ is not important here; it is enough to remind that it embeds saturation in the sense that $\phi_{A,B}$ as a function of p_T is constant for $p_T < Q_s$, where Q_s corresponds to the saturation scale. Here we show results obtained within a parameter set such that $\langle Q_s \rangle_{y=0} \approx 1$ GeV for the most central collisions at longitudinal momentum fraction $x = 0.01$.

Having described the fKLN model we are now ready to define the other two kinds of initializations we use in simulations. Firstly we assume that both the initial p_T-spectrum and the coordinate space distribution are given by equation (1) and its integral over $\boldsymbol{p}_T$, which corresponds to the proper implementation of the fKLN model. We call this initialization as fKLN initialization. This kind of initial condition is not implemented in hydro simulations because the initial strong deviation from equilibrium cannot be studied within viscous hydrodynamics. In the fKLN initialization we assume $\tau_0 = 0.2$ fm/c because no assumption on equilibration needs to be introduced; this time can be interpreted as the time needed for the strong initial fields to decay to a parton liquid, as explained in the Introduction. On the other hand, we also consider another initial condition which is close to the one usually implemented in hydro simulations, in which we assume the coordinate space distribution given by the KLN model and a p_T-thermalized spectrum. In this way we assume some thermalization occured in a short time, leaving at the same time the distribution in coordinate space unaffected. We call this initialization as Th-fKLN initialization. For the latter we assume the same initialization times used for the Th-Glauber model. In the two cases we assume $y = \eta$ at $\tau = \tau_0$.

3. Kinetic theory at fixed η/s

For the dynamical evolution of the initial conditions we employ transport theory as a base of a simulation code of the fireball expansion created in relativistic heavy-ion collision [17, 26, 18, 27]; we assume the system can be described by a gluon distribution function $f(\boldsymbol{x}, \boldsymbol{p}, t)$ which evolves according to the Relativistic Boltzmann Transport (RBT) equation:

$$p_\mu \partial^\mu f = \int d\Gamma_2 d\Gamma_{1'} d\Gamma_{2'} (f_{1'} f_{2'} - f f_2) |\mathcal{M}|^2 \delta^4(p + p_2 - p_{1'} - p_{2'}) \; , \qquad (2)$$

with $d^3\boldsymbol{p}_k = 2E_k(2\pi)^3 d\Gamma_k$, and $\mathcal{M}$ corresponds to the transition amplitude. At variance with the standard use of transport theory we have developed an approach that, instead of focusing on specific microscopic calculations of the scattering matrix, fixes the total cross section cell by cell in the grids in order to have a wished value of η/s. By means of this procedure we translate transport theory to hydrodynamical language since we use the Boltzmann equation to simulate the dynamical evolution of a fluid which dissipates with a specified shear viscosity, in analogy to what is done within hydrodynamical simulations. Hence this approach offers a bridge between transport theory and hydrodynamics.

The advantage of the kinetic theory approach at fixed η/s, compared to hydro simulations, is twofold: the initial condition does not need to be close to thermal equilibrium, because we do not perform a gradient expansion of the energy-momentum tensor. Moreover we do not need to specify an ansatz for the deviations from equilibrium. This approach to kinetic theory has been also considered in [40] where it has been shown that transport theory at fixed η/s reproduces the results of viscous hydrodynamics for one-body observable like $T^{\mu\nu}$ or entropy density also in the limit in which the system is not in the dilute regime. This is not surprising because looking at the Boltzmann collision integral in terms of viscosity allows the analytical derivation of second order viscous hydrodynamics [41, 42, 43, 44]. Despite the fact we consider only the $2 \leftrightarrow 2$ processes to compute the collision integral, once the system is close to the hydro regime with many collisions happening in a short time range, the detail of the single scattering is lost and what matters is only the viscosity of the fluid and not the specific microscopic process producing such viscosity. We have checked we work in a regime where the specific process is not relevant by changing the microscopic two-body scattering matrix from anisotropic to isotropic and adjusting the total cross section to keep the same η/s. We have found that leaving unchanged all the other parameters, the elliptic flow is not affected by this change for $p_T \leq 2.5$ GeV [45].

Once η/s is fixed, we compute the total cross section in each cell of the coordinate space of our grid. The Chapmann-Enskog approximation supplies the relation between η/s an cross section with quite good approximation, in agreement with the results obtained using the Green Kubo formula [27, 46]:

$$\sigma_{tot} = \frac{1}{15}\frac{\langle p\rangle}{\rho\, g(a)}\frac{1}{\eta/s} = \frac{1}{15}\langle p\rangle\, \tau_\eta \ , \tag{3}$$

which is valid for a generic differential cross section $d\sigma/dt \sim 1/(t - m_D^2)^2$ [46]. In the above equation $a = T/m_D$, with m_D the screening mass regulating the angular dependence of the cross section, while $g(a)$ corresponds to a function whose analytic form can be found in [19, 25]. In the regime were viscous hydrodynamic applies (not too large η/s and p_T) the specific microscopic detail of the cross section is irrelevant and our approach is an effective way to employ transport theory to simulate a fluid at a given η/s.

The η/s we use in our study [25] is as follows: in the plasma phase it is a constant, whose numerical value is fixed case by case; we then implement a kinetic freezout by assuming that η/s increases smoothly in a temperature range from the plasma phase to a hadron phase values which is fixed by referring to the estimates in [47, 48, 49]. In this way we take into account scatterings in the hadron phase as well, which however give a very tiny contribution to the collective flow because of the damping due to the larger viscosity.

4. Thermalization

In the upper left panel of figure 1 we collect the initial spectra, $dN/2\pi p_T dp_T$, integrated over the momentum rapidity window $|y| < 0.5$, for the case of a Au-Au collision $\sqrt{s} = 200A$ GeV for the fKLN and Th-Glauber initial conditions at their respective initial times τ_0 and at the final time $\tau = 8.2$ fm/c. For the case of the Th-fKLN, we find that the spectra are the same as in the case of the Th-Glauber, therefore we do not plot them in the figure. We have also shown by the dashed line the spectrum at $\tau = 1.2$ fm/c for the case of the fKLN initial condition. The results in figure 1 are obtained with $4\pi\eta/s = 1$. We notice that initially the fKLN spectrum is quite far from a thermalized spectrum; nevertheless the spectrum thermalizes in the transverse plane within 1 fm/c, since its p_T dependence becomes exponential with a slope very similar to the Th-Glauber. In [25] we have also checked thermalization is achieved in the full momentum space within $\tau_{therm} \approx 0.8$ fm/c by computing the time evolution of the quantity $T^* \equiv T\tau^{1/3}$, with $T = E/3N$ representing the temperature in the case of a thermalized system. In the case of 1D dissipation-less expansion T^* saturates to a constant as a function of time, which we find

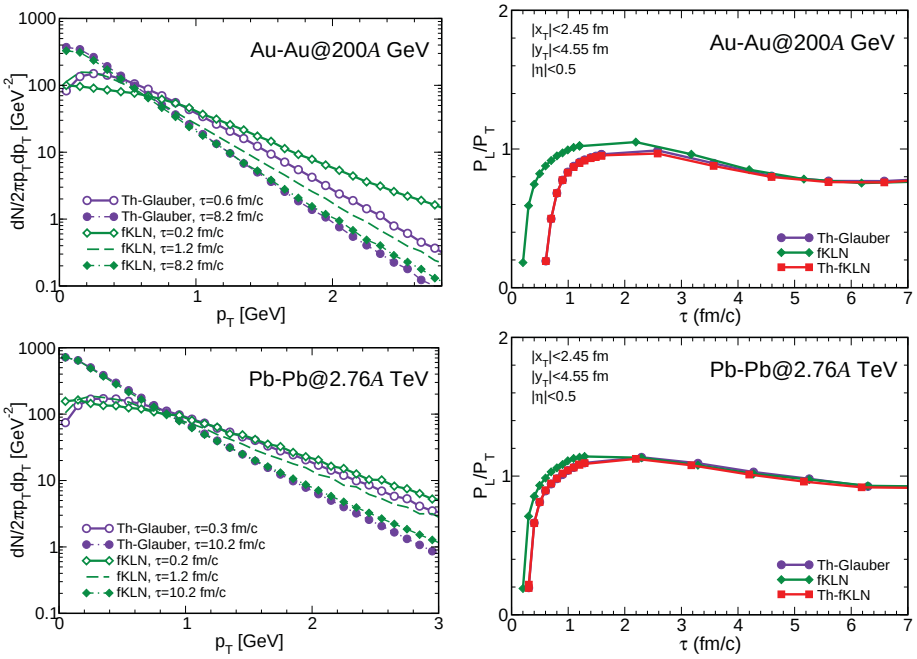

Figure 1. (Color online) Left panels: time evolution of spectra, for collisions at RHIC (upper left) and LHC (lower left) energies. Right panels: time evolution of P_L/P_T. In all panels $b = 7.5$ fm and $4\pi\eta/s = 1$. The spectra for the Th-fKLN case are not shown because we do not find visible deviations from the Th-Glauber initialization. Adapted from Ref. [25].

to happen for the fKLN case within τ_{therm}. Results for the LHC runs are shown on the lower left panel of figure 1.

On the upper right panel of figure 1, which refers to the case of Au-Au collision, we plot the ratio P_L/P_T where P_L, P_T correspond to the longitudinal and transverse pressure respectively. In the initial stage of the collision there is a strong anisotropy due to the fact that $P_L \ll P_T$; however the system efficiently removes the anisotropy in the case of small η/s, and in fact we find that the time required to get isotropic pressure $P_L \approx P_T$ is $\tau_{iso} \approx 0.3$ fm/c. In [25] we show that in case η/s is quite large and comparable with the perturbative QCD estimates, the system is not efficient in removing the initial anisotropy, which is quite natural because the large viscosity damps the flow which instead is necessary to transfer momentum and equilibrate the pressures. Results for the LHC runs are shown on the lower right panel of figure 1.

5. Elliptic flow

In the left panel of figure 2, we collect our results for the differential elliptic flow for the case of a Au-Au collision at RHIC energy with $b = 7.5$ fm. In the right panel we plot the same quantity for the case of Pb-Pb collisions at LHC energy and same impact parameter. To guide the eye, in the figure we also plot experimental data for v_2 in the relevant centrality class [50]. Since no hadronization process is yet included in our approach, the comparison with the charged hadrons v_2 has to be taken with care, even if it indicates that the azimuthal asymmetries generated by RBT are in the correct range.

Firstly we focus on the thermalized initializations, Th-Glauber and Th-fKLN. In the case of Au-Au collisions at RHIC energy, the v_2 obtained by Th-Glauber with $4\pi\eta/s = 1$ is obtained by Th-fKLN with $4\pi\eta/s \approx 2$, because momentum distribution is the same but initial eccentricity of

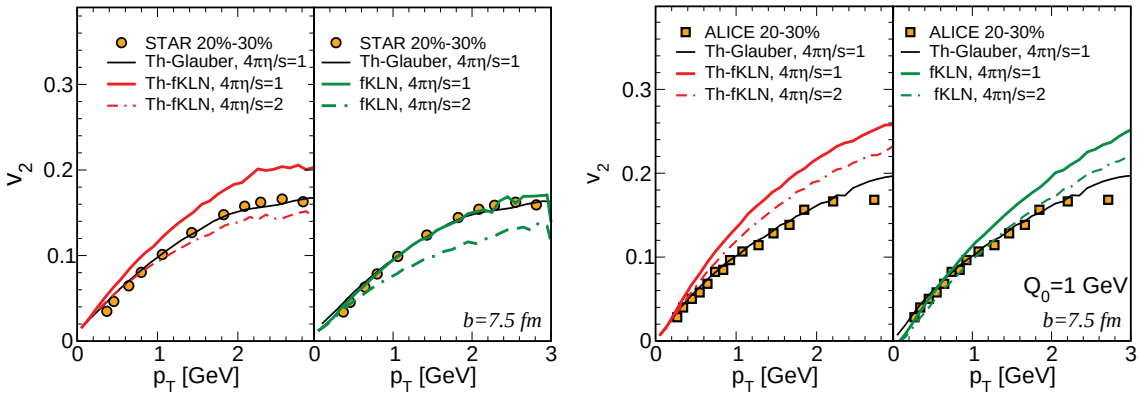

Figure 2. (Color online) Elliptic flow $v_2(p_T)$ at midrapidity $|y| < 0.5$ for different initial conditions and η/s as in the legend. Calculations in the left panel refer to Au-Au collisions at $\sqrt{s} = 200A$ GeV, while in the right panel we plot results for Pb-Pb collisions at $\sqrt{s} = 2.76A$ TeV. Adapted from Ref. [25].

Th-fKLN is larger than the one of the Th-Glauber initial condition, requiring a larger viscosity in the former case to damp the flow. These results are in agreement with the ones obtained from viscous hydrodynamics [11, 23, 24], showing the solidity and consistency of our transport approach at fixed η/s.

Next we discuss the result for the fKLN model, represented by the green lines in figure 2, with the proper distribution function implemented in both the $\boldsymbol{x}$ and $\boldsymbol{p}$ spaces. We find that fKLN with a $4\pi\eta/s = 1$ gives a $v_2(p_T)$ quite similar to the Th-Glauber, even if the initial eccentricity in this case is larger. For fKLN with $4\pi\eta/s = 2$ the differential elliptic flow would be too small. In other words the initial out-of-equilibrium fKLN distribution reduces the efficiency in converting ϵ_x into v_2. Our interpretation is that the initial large eccentricity of the fKLN configuration is compensated by the key feature of an almost saturated initial distribution in $\boldsymbol{p}$-space below the saturation scale Q_s and probably by the softer tail at $p_T > Q_s$. We obtain similar results at the LHC energy. In this case the Th-fKLN overestimate the Th-Glauber v_2 at both $4\pi\eta/s = 1$ and 2. When the full fKLN is implemented we can see that the damping effect already discussed at RHIC is such that with an $4\pi\eta/s = 2$ one is closer to the Th-Glauber with $4\pi\eta/s = 1$.

The effect we find on v_2 is more important for peripheral collisions. In fact in figure 3 we plot v_2 at $p_T = 2$ GeV for different initializations, as a function of the number of participants. This figure permits to visualize and summarize the dependence of $v_2(p_T)$ on the centrality class, comparing the impact of the initial distribution on the final v_2. We notice that the discrepancy between Th-fKLN and fKLN initializations becomes less relevant for more central collisions, implying that the effect of the initial momentum distribution is not negligible if one considers non-central collisions. We also note that for central collisions at RHIC Th-Glauber and Th-fKLN for $4\pi\eta/s = 1$ predict the same v_2 and the effect is of KLN generating larger v_2 disappears. This is seen also in viscous hydro simulation and it is a further confirmation that our approach converge to viscous hydro when the same thermal initial conditions are employed.

6. Conclusions

In this contribution we have reported our results [19, 25] on thermalization and building-up of the elliptic flow for fireballs produced in relativistic heavy ion collisions both at RHIC and LHC energies. We have put emphasis on the role of a nonequilibrium initial condition on the generation of the collective flow, when the KLN initialization is properly implemented in

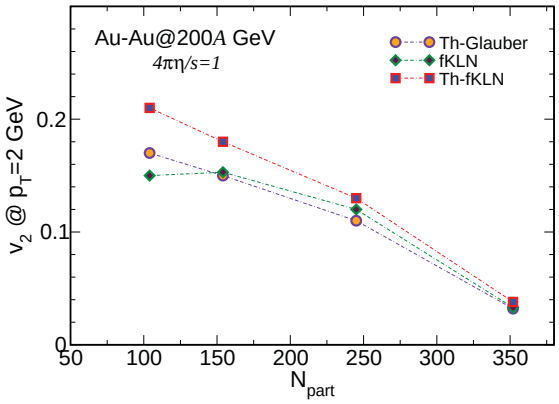

Figure 3. (Color online) Elliptic flow $v_2(p_T)$ at midrapidity $|y| < 0.5$ and at $p_T = 2$ GeV for different initial conditions, computed at $4\pi\eta/s = 1$. All the calculations refer to Au-Au collisions at $\sqrt{s} = 200$ GeV. Adapted from Ref. [25].

coordinate and momentum space. Our study is based on kinetic theory at fixed η/s. Fixing the shear viscosity over entropy density ratio permits to forget about microscopic processes which give that specific value of the ratio itself, and to focus on the effect of shear viscosity on thermalization, isotropization and building of the collective flows.

For what concerns thermalization, in both RHIC and LHC runs we have found that thermalization times are $\tau_{therm} \approx 0.8$-1 fm/c. We have then focused our attention on the elliptic flow production when the initial distribution has a saturation scale built in it. We have found that the amount of elliptic flow produced in heavy ion collisions depends not only on the pressure gradients and the η/s of the system, but also on the initial distribution in momentum space. In particular, an initial condition characterized by a momentum distribution with a saturation scale generates smaller v_2 respect to the thermal one. Assuming the fKLN distribution as the one arising from the shattering of the CGC, the effect of the initial nonequilibrium distribution affects the estimate of η/s of about a factor of two. However we have also that this effect is maximal for semi-peripheral collisions, becoming quite small for very central collisions.

In order to make more precise comparison with experimental data we are currently implementing also fluctuating initial conditions which will allow to extend the present study to all the v_n harmonics relevant in HIC's. This will allow to see if fKLN can account for the measured v_3 or the non-equilibrium damps such harmonics even more than what seen in hydrodynamics. In [51] it is found that harmonics up to the fifth order can be reproduced by combining CYM early-time with hydro late-evolution evolutions; however in the calculations of [51] a small deviation from equilibrium has to be assumed in order to use viscous hydrodynamical equations. Therefore it will be interesting to compute the higher order harmonics combining the CYM initial spectrum with the dynamics embedded in the kinetic equations where the assumption of sudden thermalization can be relaxed, which will be the subject of future studies.

Acknowledgments

V G and F S acknowledge the ERC-STG funding under the QGPDyn grant.

References

[1] Adams J *et al.* [The STAR Collaboration] 2005 *Nucl. Phys. A* **757** 102; Adcox K *et al.* [The PHENIX Collaboration] 2005 *Nucl. Phys. A* **757** 184
[2] Aamodt K *et al.* [The ALICE Collaboration] 2010 *Phys. Rev. Lett.* **105** 252302

[3] Jacak B and Muller B 2012 *Science* **337** 310
[4] Fries R *et al.* 2008 *Ann. Rev. Nucl. Part. Sci.* **58** 177
[5] Csernai L *et al.* 2006 *Phys. Rev. Lett.* **97** 152303
[6] Lacey R *et al.* 2007 *Phys. Rev. Lett.* **98** 092301
[7] Kovtun D *et al.* 2005 *Phys. Rev. Lett.* **94** 111601
[8] Ollitrault J Y 1992 *Phys. Rev. D* **46** 229
[9] Romatschke P and Romatschke U 2007 *Phys. Rev. Lett.* **99** 172301
[10] Song H and Heinz W W 2008 *Phys. Rev. C* **78** 024902
[11] Song H *et al.* 2011 *Phys. Rev. C* **83** 054910
[12] Schenke B *et al.* 2010 *Phys. Rev. C* **82** 014903
[13] Niemi *et al.* 2011 *Phys. Rev. Lett.* **106** 212302
[14] Xu Zand Greiner C 2009 *Phys. Rev. C* **79** 014904
[15] Xu Z, Greiner C, and Stocker H 2008 *Phys. Rev. Lett.* **101** 082302
[16] Bratkovskaya E *et al.*2011 *Nucl. Phys. A* **856** 162
[17] Ferini G, Colonna M, Di Toro M, and Greco V 2009 *Phys. Lett. B* **670** 325
[18] Plumari S and Greco V 2012 *AIP Conf. Proc.* **1422** 56
[19] Ruggieri M *et al.* 2013 *Phys. Lett. B* **727** 177
[20] Uphoff J *et al.* 2014 `arXiv:1401.1364`
[21] McLerran L and Venugopalan R 1994 *Phys. Rev. D* **49** 2233; 1994 *Phys. Rev. D* **49** 3352; 1994 *Phys. Rev. D* **50** 2225
[22] Alver B *et al.*2010 *Phys. Rev. C* **82** 034913
[23] Adare A *et al.* [The PHENIX Collaboration] 2011 *Phys. Rev. Lett.* **107** 252301
[24] Luzum M and Romatschke P 2008 *Phys. Rev. C* **78** 034915
[25] Ruggieri M et al. 2013 `arXiv:1312.6060`
[26] Plumari S *et al.* 2010 *Phys. Lett. B* **689** 18
[27] Plumari S *et al.* 2013 *J. Phys. Conf. Ser.* **420** 012029
[28] Kharzeev D, Levin E, and Nardi M 2005 *Nucl. Phys. A* **747** 609; Kharzeev D, Levin E, and McLerran L 2003 *Phys. Lett. B* **561** 93; Kharzeev D and Nardi M 2001 *Phys. Lett. B* **507** 121; Kharzeev D and Levin E 2001 *Phys. Lett. B* **523** 79; Hirano T and Nara Y 2004 *Nucl. Phys. A* **743** 305
[29] Hirano T *et al.* 2006 *Phys. Lett. B* **636** 299
[30] Drescher W and Nara U 2007 *Phys. Rev. C* **75** 034905; 2007 *Phys. Rev. C* **76** 041903
[31] Hirano T and Nara Y 2009 *Phys. Rev. C* **79** 064904
[32] Drescher H *et al.* 2006 *Phys. Rev. C* **74** 044905
[33] Shen C *et al.* 2013`arXiv:1308.2440`
[34] Shen C*et al.* 2013 `arXiv:1308.2111`
[35] Song H *et al.* 2013 `arXiv:1311.0157`
[36] Ryblewski R and Florkowski W 2013 *Phys. Rev. D* **88** 034028
[37] Gelis F and Epelbaum T 2013 `arXiv:1307.2214`
[38] Fukushima K 2013 `arXiv:1307.1046`
[39] 2007 Miller M L *et al.Ann. Rev. Nucl. Part. Sci.* **57** 205
[40] Huovinen P and Molnar D 2009 *Phys. Rev. C* **79** 014906
[41] Grad H 1949 *Commun. Pure Appl. Math.* **2** 331; 1949 *Commun. Pure Appl. Math.* **2** 325
[42] Denicol G *et al.* 2012 *Eur. Phys. J. A* **11** 170g
[43] Tsumura K and Kunihiro T 2013 `arXiv:1311.7059`
[44] Bazow D *et al.* 2013`arXiv:1311.6720`
[45] Greco V 2013 *Anisotropic Flow from a Kinetic Theory Approach* talk given at INPC 2013, 2-6 June 2013, Florence (Italy)
[46] Plumari S *et al.* 2012 *Phys. Rev. C* **86** 054902
[47] Prakash M *et al.* 1993*Phys. Rep.* **227** 321
[48] Chen *et al.* 2007 *Phys. Rev. D* **76** 114011
[49] Demir N and Bass S 2009 *Phys. Rev. Lett.* **102** 172302
[50] Adams J *et al.* [The STAR Collaboration] 2005 *Phys. Rev. C* **72** 014904; Dobrin A 2011 *J. Phys. G* **38** 124170
[51] Gale C*et al.* 2013 *Phys. Rev. Lett.* **110** 012302
[52] Song H and Heinz U 2008 *Phys. Lett. B* **658** 279